UNEC Journal of Engineering and Applied Sciences
Vol. 6, No.1, 2026, pp. 100-107
DOI: https://doi.org/10.61640/ujeas.2026.0509

SECTION:
CHEMISTRY &
MATERIAL SCIENCES

Synthesis and structure investigation of new complexes of silver nanoparticles with -(4-fluorophenyl) diazen-1-yl) benzene-1,2,3-triol and cetylmetylammonium bromide

A.A. Imamaliyeva[1*], F.M. Chiraqov[1], F.V. Hajiyeva[1]

[1]Baku State University, 23 Zahid Khalilov Street, Baku AZ1148, Azerbaijan
email: *aytenimamaliyeva@hotmail.com*

Abstract

Novel binary (Ag/R) and ternary (Ag/R/CTAB) complexes were prepared using eco-friendly synthesized silver nanoparticles (AgNPs), an azo derivative ligand—4-(2-(4-fluorophenyl) diazen-1-yl) benzene-1,2,3-triol (R) and cetyltrimethylammonium bromide (CTAB). XRD analysis revealed the formation of a crystal structure in both binary and ternary complexes. In the binary complex, the main diffraction peaks were observed at 19.42°, 38.08°, 44.24°, 64.42°, 77.28° and 81.46°. In the ternary complex, peaks were recorded at 21.39°, 30.82° and 44.36°. UV-vis analyses showed significant shifts in the absorption bands, which indicate that the electronic transitions changed during the formation of the complexes. The main peaks of the R reagent were observed at 216, 365 and 432 nm, and after combining with Ag, these values changed to 201, 276 and 416 nm. When CTAB was added, peaks were recorded at 207, 237 and 276 nm. IR results showed the main functional groups involved in the structure of the complex. Vibrations related to O-H, C=O and Ar-N=N-Ar groups were clearly observed in the spectra. In addition, the formation of Ag-O bonds was confirmed in the region between 570, 544 and 515 cm^{-1}. Overall, the obtained results indicate that both binary and ternary complexes were successfully synthesized and that they are structurally stable.

***Keywords*:** nanomaterials, eco-friendly synthesis, coordination complex, azo reagent.
PACS numbers: 61.46-w, 78.67. Bf, 61.05.-cp, 81.07.-b, 82.80-Ej

Received:	*Revised:*	*Accepted:*	*Published:*
16 May 2025	*20 November 2025*	*6 April 2026*	*31 May 2026*

1. Introduction

In recent years, combined use of nanoparticles with azo reagents has attracted a lot of attention. This combination makes the system very stable and expands its functional properties. Azo groups prevent nanoparticles from aggregation and increase the stability of the system. At the same time, the N=N groups in their structure are distinguished by strong color characteristics [1-7]. These types of properties of nanoparticles are mainly related to their surface area and the limited movement of electrons. Silver nanoparticles are widely used not only in optics but also in fields such as photocatalysis, photonics and information storage, their high optical responsivity makes them suitable for use in colorimetric sensors [7-15]. In literature, a number of studies have been conducted in this field. For example, Hassanpoor and his colleagues have developed a highly sensitive spectrophotometric method for the determination of Uranium (VI) ions [16]. Kaushal Kumar compared the antibacterial properties of nanoparticles, while Minjie showed the relationship between the shape of the particles and their activity [17]. Minjie et al. synthesized silver nanoparticles with various

controlled shapes and investigated the effect of these shapes on their antibacterial properties. As a result, it was found that the morphology of the nanoparticles plays an important role in their antimicrobial efficacy [18]. The main objective of this study is the synthesis of new binary and ternary complexes based on AgNPs, an azo derivative reagent, and CTAB. At the same time, the use of these complexes in the determination of ions and the effect of azo compounds and CTAB on the stability and efficiency of the system were studied. The structure, synthesis and properties of the obtained complexes were investigated by various analytical methods, including spectrophotometry, X-ray diffraction and infrared spectroscopy. In addition, the combined use of AgNPs and CTAB was evaluated to determine how the stability, sensitivity, and electronic properties of the complexes were modified. The results obtained show that this approach opens up new possibilities for more accurate and reliable determination of ions and other analytes and has promising applications in the fields of catalysis, sensing, and analytical chemistry [19-21]. The main purpose of this work is to obtain new complexes of nanoparticles with azo coupling and CTAB, and to study the binary and ternary complexes obtained by various methods. The results show that the combined use of CTAB and silver nanoparticles increases both the stability and sensitivity of the system and creates opportunities for more effective analytical applications. The findings suggest that these complexes hold promise for the development of efficient and reliable detection methods for a wide range of ions and other analytes.

2. Experiments

Materials

Silver nitrate ($AgNO_3$, PLC 141459, 98% chemically pure), cetyltrimethylammonium bromide (CTAB, AB 117004), β-D glucose ($C_6H_{12}O6$, CAS No.50-99-7); sodium hydroxide (NaOH, PLC 1416x87), soluble starch ($(C_6H_{10}O_5)n$, PLC 121096, 98% chemically pure), ethanol (C_2H_5OH, CAS No.64-17-5, 95%), benzidine ($C =_{12}H_{12}N_{2}$, CAS No.92-87-5), sodium nitrite ($NaNO_2$, CAS No.7632-00-0), hydrochloric acid (HCl, CAS No.-01-0), were used employed in this study.

Research methods.

The crystal structure of the synthesized silver nanoparticles and their complexes with the pyrogallol-based reagent were analyzed using X-Ray diffraction on a Rigaku Mini Flex 600 diffractometer an ambient condition. The UV spectra and optical properties of Ag nanoparticles and silver-based complexes were studied using an ultraviolet spectrophotometer (Specord 210) at room temperature over within the spectral range of 200-900 nm. IR spectra of samples were measured on an infrared spectrometer Varian 640-IR at wavelength 400-4000 cm-1 at room temperature.

Preparation of Ag nanoparticles.

The formation of Ag nanoparticles begins with the preparation of solutions containing key reagents. A 1% starch solution is combined with a 0.01 M $AgNO_3$ solution, followed by the addition of a mixture comprising 0.2 M glucose and 0.07 M NaOH solutions. The obtained solution is mixed for 30 minutes. During this period, the color of the solution becomes dark brown, which indicates that the colloidal solution of silver nanoparticles has formed [18-20]. It is then processed in an R 5430 Eppendorf ultracentrifuge operating at 12,000 rpm to ensure the stability of the nanoparticles and to remove residual ions. Afterward, the nanoparticles are washed multiple times using an aqueous-ethanol solution. It is noteworthy that throughout the synthesis process, the dissolved starch plays function as both a reductant and a stabilizing agent. Sodium hydroxide (NaOH) functions as an activating agent, facilitating the reaction kinetics, where glucose plays the role as a reducing agent, contributing to the formation of Ag nanoparticles [22].

Synthesis of 4-2-(4fluorphenol) diazen-1) benzene-1,2,3 triol reagent.

To diazotize parafluoroaniline (PFA), add 2.48 g (0.01 mol) of it to a 500 ml three-necked flask and dissolve it in 2.5 ml of measured volume of hydrochloric acid solution. The system was maintained at o low temperature until reaching 0°C with ice and solution of 0.69 g (0.01 mol) was added dropwise a of $NaNO_2$ in 5 mL of water while stirring with a mechanical stirrer, leading to the formation of the diazonium salt. If the temperature of the system rises above 0°C, ice cubes are incorporated to the mixture. Carry out diazotization reaction at 0°C for 30 min. Add a small amount of urea to the solution to remove excess sodium nitrite. Add 1.26 g (0.01 mol) of pyrogallol to a 500 ml three-necked flask and dissolve it in 10 ml of pH 3 solution. Reduce the temperature of the mixture to 0°C and supply the diazonium solution by slow addition while stirring with a mechanical stirrer. Carry out the synthesis reaction of the azo compound for 1.5-2 hours. The obtained colored precipitate is filtered through a vacuum filtration setup, rinsed with distilled water, purification by recrystallization, and dried in a desiccator filled with CaCl2. The yield is 76%.

Preparation of Ag/R/CTAB based complex.

In this article, we explore the formation of the Ag/R/CTAB-based complex, where Ag represents silver nanoparticles, R denotes a pyrogallol-based azo compound, and CTAB functions as a stabilizing agent. The synthesis method commences with the preparation of the pyrogallol-based azo compound, synthesized using a method documented in the literature. The reagent, with a concentration of 10^{-3} M, is accurately measured and dissolved in an alcohol-water solution. Subsequently, the obtained sample is moved to a 100 mL measurement flask. Following this, 50 ml of the reactive solution is poured to a 100 mL glass vessel. To this solution, 10 ml of Ag nanoparticles with a concentration of 0.01 M are added, and the solution is continuously stirred for 2 hours. The color change that occurs at the beginning indicates the formation of a coordination bond as the first stage of synthesis. After that, 5 ml of CTAB is added to the obtained binary complex, and stirring is continued for 2 hours. At this stage, a color change occurs again, which indicates the formation of a ternary system. The obtained complexes are dried at 180 degrees in 3 hours to reduce the amount of solvent and moisture. [23-25].

3. Results and discussion

In figure 1, the X-ray diffraction patterns of the complexes formed by silver nanoparticles (AgNPs) with azo-based reagents are presented. X-ray diffraction (XRD) was utilized to examine the crystal configurations of AgNPs and their complexes. crystalline structure distinct peaks are observed, where amorphous or non-crystalline materials display diffuse and weak patterns. The Debye-Scherrer equation (1) was applied to determine the crystallite sizes of the reagent binary and ternary complexes.

$$D = \frac{K\lambda}{\beta COS\theta} \quad (1)$$

In this equation K represents a constant (K=0,94), λ denotes the X-ray wavelength (λ=1.5406 Å,C_u Kα radiation), θ- corresponds the diffraction angle.

In figure 1b, sharp diffraction peaks are observed at 2θ = 19.42°, 38.08°, 44.24°, 64.42°, 77.28°, and 81.46°, which correspond to the planes of the binary complex formed by the reagent with silver. In figure 1c when CTAB is added as a third component, new peaks appear at 2θ = 21.39°, 30.81°, and 44.36°, corresponding to additional planes. The broadening of the peaks indicates that the crystals are very small in size. Based on the XRD diffractograms, the average crystal size in the Ag/R binary complex is calculated to be 10.09 nm, while in the Ag/R/CTAB ternary complex, the average crystal size increases to 19.2 nm.

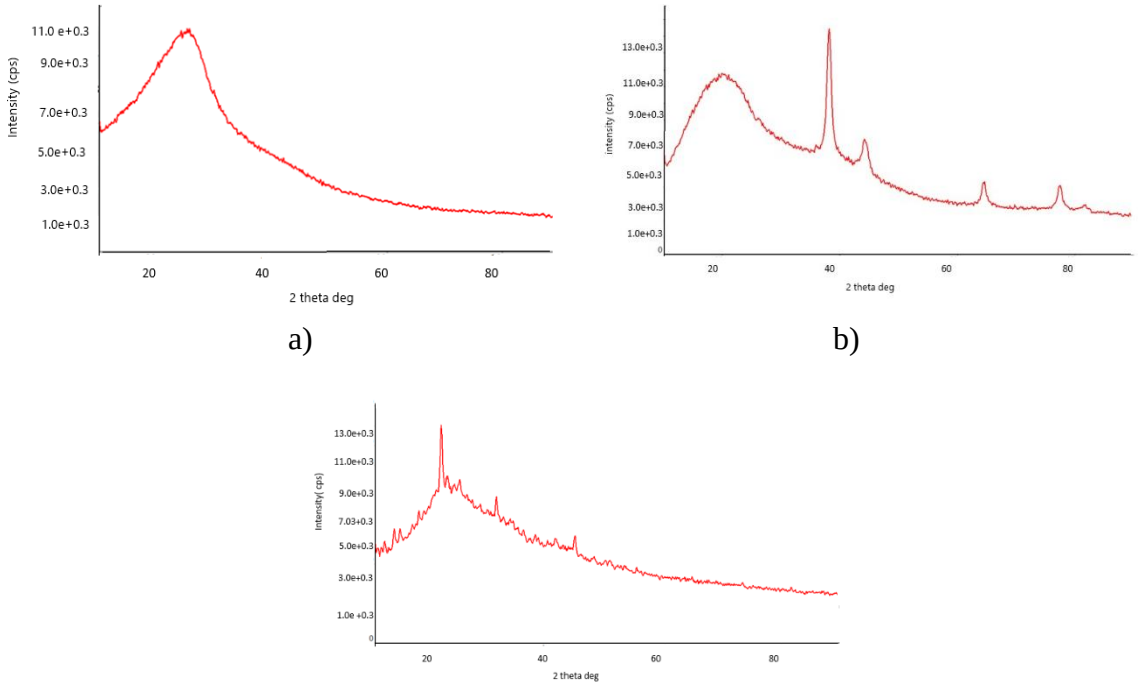

Figure 1. Diffraction patterns of reagent R (a), binary Ag/R (b) and ternary Ag/R/CTABr (c) complexes

In figure 1b, sharp diffraction peaks are observed at 2θ = 19.42°, 38.08°, 44.24°, 64.42°, 77.28°, and 81.46°, which correspond to the planes of the binary complex formed by the reagent with silver. In figure 1c when CTAB is added as a third component, new peaks appear at 2θ = 21.39°, 30.81°, and 44.36°, corresponding to additional planes. The broadening of the peaks indicates that the crystals are very small in size. Based on the XRD diffractograms, the average crystal size in the Ag/R binary complex is calculated to be 10.09 nm, while in the Ag/R/CTAB ternary complex, the average crystal size increases to 19.2 nm.

Ag/R			Ag/R/CTAB		
2θ	β	D, nm	2θ	β	D, nm
19.42^0	9.53	0.88	21.39^0	0.44	19.2
38.080^0	0.87	10.09	30.81^0	0.34	25.32
44.24^0	1.45	6.18	44.36^0	0.44	20.37
64.42^0	0.84	11.68			

Table 1. X-ray diffraction (XRD) parameters of binary and ternary complexes

Infrared (IR) spectroscopy for silver nanoparticles can reveal information about the capping agents or stabilizing ligands surrounding the nanoparticles. The IR spectra of the AgNPs combined with the azo-based reagent display characteristic peaks corresponding to the chemical groups existing in the stabilizing agents. As depicted in Figure 2 a, the IR spectrum of the R reagent displays well defined absorbsion band in the 3800–3000 cm^{-1} and 500–1800 cm^{-1} regions. The reagent contains aromatic rings, hydroxyl (–OH), and azo (–N=N–) functional groups. In the spectrum of compound R, a wide absorbsion band observed in the region of 3386–3390 cm^{-1} is assigned to the O–H vibration. The shift of this signal to approximately 3400 cm^{-1} in the Ag/Rg complex, along with a decrease in its intensity, indicates the coordination of hydroxyl groups with silver nanoparticles. The characteristic signal of the azo group (–N=N–) shifts from 1443 cm^{-1} to 1451 cm^{-1} upon the addition of

silver, confirming that this functional group also participates in interaction with the metal. The absorption band belonging to the aromatic C=C system moves from 1607 cm^{-1} to 1614 cm^{-1}. This change indicates that the electron distribution sharing in the molecule has changed and the interaction effect with silver has occurred. The band belonging to the C-O group also moves from 1274 cm^{-1} to 1281 cm^{-1}. which in this case is related to the formation of metal-ligand bond and changes in hydrogen bonding. In the range of 500-600 cm^{-1}, the formation of new weak peaks at 530 cm^{-1} and 525 cm^{-1} confirms the formation of coordination interactions with silver. In the spectrum of the ternary complex (Ag/R/CTAB), these changes are even more pronounced, indicating that CTAB enhances the stability of the complex and induces additional structural modifications. In the study by Lutsenko A. et al. the structures and IR spectra of Ag^{+}–phenol complexes were investigated in the gas phase using photodissociation spectroscopy and quantum chemical methods. The results indicate that Ag^{+} ions form coordination bonds with the functional groups of phenol molecules, leading to spectral changes [27]. Wang et al reported that azo dye-stabilized silver nanoparticles exhibit IR spectral shifts in the N=N and O–H vibration regions, indicating specific interactions between the azo groups and the nanoparticle surface [28]. Kvítek et al. demonstrated that phenolic and aromatic amine groups serving dual roles as both reducing and stabilizing agents during silver nanoparticle formation, causing notable shifts in IR bands associated with these functional groups [29,30].

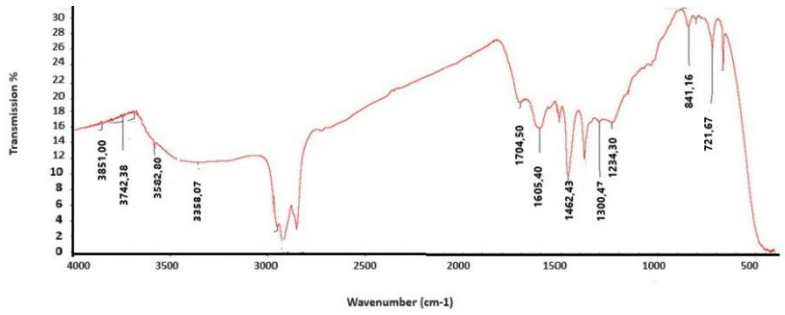

a)

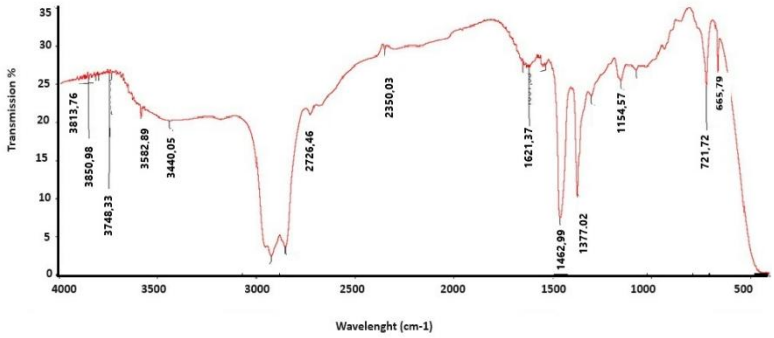

b)

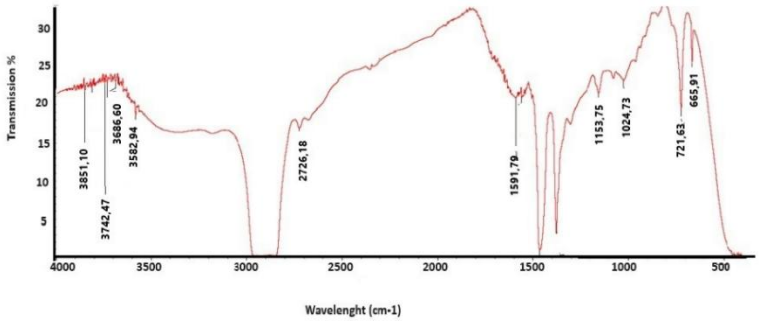

c)

Figure 2. IR spectra of reagent R (a), binary Ag/R (b) and ternary Ag/R/CTABr (c) complexes

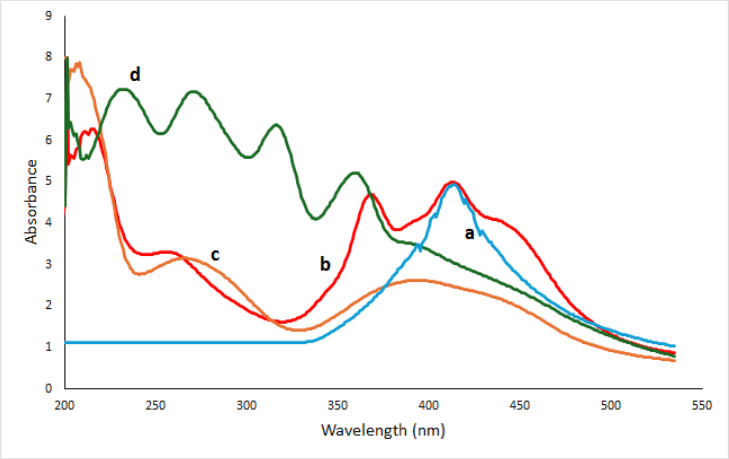

Figure 3. UV spectra of Ag nanoparticles (a), reagent R (b), binary Ag/R (c) and ternary complexes Ag/R/CTAB (d)

UV-V is spectroscopy of silver is an effective method for studying the optical properties of complexes resulting from the interaction between silver nanoparticles (AgNPs) and azo compounds. In the UV spectra of silver nanoparticles, it has been determined that the maximum intensity of the absorption bands of silver nanoparticles vary between 400-450 nm supporting on their scale. Figure 3 demonstrates that the Uv absorbsion spectrum of reagent R spans 200-500 nm, showing maxima at 218,369 and 412 nm, which correspond to transitions of C-C bonds and n-p transitions of C=N functionalities. When 0.01 M concentrated silver nanoparticles are added to the reagent solution, the absorption curves of the resulting binary complex move to the lower wavelength relative to the peak at 416 nm of the Ag nanoparticle, resulting in the appearance of new maximum peaks at 201 nm, 276 nm, and 416 nm. The formation of the Ag-R nanocomposite is accompanied by a visible color transition from dark brown to yellow confirming complex formation. The addition of CTAB as a stabilizing agent to the Ag nanoparticle-R reagent system leads to the formation of a ternary system. This results in noticeable spectral changes, where the absorption maxima of the ternary system are shifted toward shorter wavelength compared to the reagent. This hypochromic shift can be attributed to quantum size effects. The interaction between ag nanoparticles and the reagent I the presence of a surfactant results in new absorption features associated with surface plasmon resonance. In addition, the system exhibits a color change from dark brown to light yellow, which is related to nanoparticles aggregation. This aggregation also causes a hypochromic shift, with the peak shifting to a smaller wavelength. In Figure 3, the shift of the silver nanoparticle spectrum, marked by 1, compared to the spectra of the reagent and the complexes, is associated to the intensity of the silver plasmon resonance. Based on this, it can be concluded that the plasmon frequency of silver is higher in the case of the binary and ternary complexes compared to the unmodified Ag nanoparticle.

4. Conclusion

In this work, binary and ternary complexes were synthesized based on silver nanoparticles in the presence of a pyrogallol reagent (R) and cetyltrimethylammonium bromide (CTAB), an azo derivative. Based on the X-ray diffraction results, the observation of peaks at angles 2θ = 19.42°, 38.08° and 44.24° in binary complexes, and 2θ = 21.39°, 30.81° and 44.36° in ternary complexes indicates that they have a crystalline structure. During the infrared spectroscopy analysis, the signals of the main functional groups involved in the complexation, –O–H, –C=O and C=C, as well as the bands corresponding to the Ag–O bonds in the regions of 570, 515 and 544 cm^{-1} were recorded, which confirms the complexation

process. In the UV-Vis spectrum, it is clearly seen that the position of the absorption maxima has changed. For the binary complex, peaks were determined at 201 nm, 276 nm and 416 nm, and for the ternary complex, these peaks were determined at 207 nm, 237 nm and 276 nm. The change in the color of the solution from dark brown to yellow also confirms the formation of the Ag–R-based nanocomposite. As a result, these complexes have crystal structures and are resistant to oxidation.

References

1. M. G. Minjie, S. Lei, W. Zhiqiang, Zh. Yanbao, Mater. Sci. Eng. C **33**(1) (2013) 397.
2. S. Agnihotri, S. Mukherji, S. Mukherji, RSC Adv. **4**(8) (2014) 3974.
3. M. Aaliya, K. Naeem, N. Jamila, S. Khan, A. Ali, Arab. J. Chem. **13**(12) (2020) 8898.
4. W. Hong, Z. Guobing, M. Rony, W. Wei, X. Linlin, L. Shaofang, M. Sakil, L. Huihong, J. Alloys Compd. **894** (2022) 162502.
5. K. Vijay, S. Devendra, M. Sweta, B. Daraksha, K.G. Ravi, H.H. Syed, J. Photochem. Photobiol. B **168** (2017) 67.
6. S. Sattar, G. Khayatian, RSC Adv. **11**(6) (2021) 3295.
7. Z.A. Ratan, M.F. Haidere, Md. Nurunnabi, Md.S. Sadi, A.J.S. Ahammad, Y.Y. Shim, M.J.T. Reaney, J.Y. Cho, Cancers **12**(4) (2020) 855.
8. M. Baghirov, M. Muradov, G. Eyvazova, S. Mammadyarova, Y. Azizian-Kalandaragh, N. Musayeva, E. Gasimov, F. Rzayev, RSC Adv. **14**(24) (2024) 16696.
9. K. Kaushal, R. Satyesh, K. Mithun, N. Mishra, S.P. Shrivastava, J. Indian Chem. Soc. **100**(4) (2023) 100965.
10. T. Kisyelov, A. Novruzova, F. Hajiyeva, M. Ramazanova, A. Chianese, Chem. Eng. Trans. **47** (2016) 121.
11. O. Acar, O.M. Kalfa, O. Yalçınkaya, A.R. Türker, Anal. Methods **5**(3) (2013) 748.
12. E.A. Terenteva, V.V. Apyari, E. Kochuk, S. Dmitrienko, Yu.A. Zolotov, J. Anal. Chem. 72 (2017) 1138.
13. D. Vilela, M. González, A. Escarpa, Anal. Chim. Acta **751** (2012) 24.
14. L. Liang, Q. Liu, G. Wang, Trends Anal. Chem. **37** (2012) 32.
15. G. Khayatian, S. Hassanpoor, A.R.J. Azar, S. Mohebbi, J. Braz. Chem. Soc. **24** (2013) 1808.
16. K. Kaushal, R.A. Satyesh, P. Himanshu, K. Mithun, N. Mishra, S.P. Shrivastava, J. Indian Chem. Soc. **100** (2023) 1965.
17. G. Minjie, S. Lei, W. Zhiqiang, Zh. Yanbao, Mater. Sci. Eng. C **33**(1) (2013) 397.
18. E. Oliveira, C. Nunez, H.M. Santos, L. Santos, J. Fernández-Lodeiro, A. Fernández-Lodeiro, J.L. Capelo, C. Lodeiro, Sens. Actuators B Chem. **212** (2015) 297.
19. M. An'amt, P. Rameshkumar, N. Huang, L.S. Wei, Microchim Acta **183**(2) (2015).
20. C. Ng, P. Chen, M. Sivakumar, Chem. Eng. Res. Des. **51**(15) (2012) 5375.
21. Sh. Behzadi, F. Ghasemi, M. Ghalkhani, A.A. Ashkarran, S.M. Akbari, S. Pakpour, M.R. Hormozi-Nezhad, Z. Jamshidi, S. Mirsadeghi, R. Dinarvand, F. Atyabi, M. Mahmoudi, Nanoscale **7**(12) (2015) 5134.
22. A.A. Imamaliyeva, F.V. Hajiyeva, F.M. Chiragov, UNEC J. Eng. Appl. Sci. **4**(2) (2024) 12.
23. H. Bahrulolum, S. Nooraei, N. Javanshir, H. Tarrahimofrad, V.S. Mirbagheri, A.J. Easton, G. Ahmadian, J. Nanobiotechnol. **19**(1) (2021) 86.
24. R. Mariselvam, A.J.A. Ranjitsingh, P. Mosae Selvakumar, A.A. Alarfaj, K. Kannan, Bioinorganic Chemistry and Applications **2016** (2016) 8629178.
25. M.A. Jafarov, V.M. Salmanov, A.H. Huseynov, R.M. Mamedov, T.A. Mamedova, F.S. Ahmedova, A.B. Aliyeva, UNEC J. Eng. Appl. Sci. **3**(2) (2023) 54.
26. T.G. Naghiyev, E.M. Huseynov, UNEC J. Eng. Appl. Sci. **3**(1) (2023) 10.
27. U.N. Naghiyeva, S.R. Hajiyeva, F.V. Hajiyeva, UNEC J. Eng. Appl. Sci. **5**(1) (2025) 83.

28. D. Hu, J. Lin, Sh. Jin, Y. Hu, W. Wang, R. Wang, B. Yang, Mater. Chem. Phys. **170** (2016) 108.
29. R. Irudhaya, N. Singh, S. Dadan, Sh. A, Sonter, K. Khemchand, P.K. Singh, A. Jaiswal, J. Bionanosci. **12**(3) (2018) 390.
30. A.O. Mekhrabov, E.A. Irmak, M.V. Akdeniz, R.M. Rzaev, UNEC J. Eng. Appl. Sci. **5**(1) (2025) 43.